Eur. Phys. J. C (2014) 74:2830
DOI 10.1140/epjc/s10052-014-2830-6

THE EUROPEAN PHYSICAL JOURNAL C

Regular Article - Theoretical Physics

Exotic $J^{PC} = 1^{-+}$ mesons in a holographic model of QCD

L. Bellantuono[1,2], **P. Colangelo**[1], **F. Giannuzzi**[1,2,a]

[1] INFN-Sezione di Bari, via Orabona 4, 70126 Bari, Italy
[2] Dipartimento di Fisica, Universitá degli Studi di Bari, via Orabona 4, 70126 Bari, Italy

Received: 28 February 2014 / Accepted: 18 March 2014 / Published online: 9 April 2014

Abstract Mesons with quantum numbers $J^{PC} = 1^{-+}$ cannot be represented as simple quark–antiquark pairs. We explore hybrid configurations in the light meson sector comprising a quark, an antiquark and an excited gluon, studying the properties of such states in a phenomenological model inspired by the gauge/gravity correspondence. The computed mass, compared to the experimental mass of the 1^{-+} candidates $\pi_1(1400)$, $\pi_1(1600)$ and $\pi_1(2015)$, favours $\pi_1(1400)$ as the lightest hybrid state. An interesting result concerns the stability of hybrid mesons at finite temperature: they disappear from the spectral function (i.e. they melt) at a lower temperature with respect to other states, light vector and scalar mesons and scalar glueballs.

1 Introduction

There are combinations of spin, parity and charge conjugation of meson quantum numbers that cannot be obtained by a quark model description of a quark–antiquark pair with orbital angular momentum L and quark spin S_q and $S_{\bar{q}}$. This is the case of the J^{PC} "exotic" combinations 0^{--}, 0^{+-}, 1^{-+}, etc. Nevertheless, hadrons with those quantum numbers were envisaged since the early high energy theoretical and experimental investigations [1], and their search has continued till the present days. An argument in favour of the existence of the exotic resonances is that they could be obtained by adding a gluonic excitation to the $q\bar{q}$ pair, and therefore they represent a "hybrid" $qG\bar{q}$ state with the unconventional J^{PC} allowed. Such exotic hybrid configurations should be observed as additional states in the meson spectrum.

From the experimental side, investigations in the heavy quark sector have reported of several mesons with nonconventional features; however, there is no observation (so far) of states with exotic quantum numbers [2]. On the other hand, in the light quark sector there are at least three quite well established hybrid candidates: $\pi_1(1400)$, $\pi_1(1600)$ and $\pi_1(2015)$.

The $J^{PC} = 1^{-+}$ state $\pi_1(1400)$ has been reported by the E852 Brookhaven experiment [3,4] in the process $\pi^- p \to \eta\pi^- p$; it was introduced to explain an asymmetry in the $\eta\pi$ angular distribution which could indicate an interference between $\ell = 1$ and $\ell = 2$ partial waves. Other analyses are described in Refs. [5–8]. The measured mass is $M(\pi_1(1400)) = 1354 \pm 25$ MeV [9].

$\pi_1(1600)$, again with $J^{PC} = 1^{-+}$, has been also reported in $\pi^- p$ interactions [10–14] with mass $M(\pi_1(1600)) = 1662^{+8}_{-9}$ MeV [9]. However, the CLAS Collaboration at JLab searched this state through the photoproduction process $\gamma\, p \to \pi^+\pi^+\pi^-(n)$, without finding evidence of it [15].

The third state with $J^{PC} = 1^{-+}$, the meson $\pi_1(2015)$, has been reported by the E852 Collaboration in Refs. [12,13]. A second peak in $\pi^- p$ interaction has been observed at about 2001 MeV in $f_1\pi$ final state, which is absent in the $\eta\pi$, $\eta'\pi$ and $\rho\pi$ final states, and this represents a new hybrid meson candidate [12]. The signal has also been seen in $b_1(1235)\pi^-$ at about 2014 MeV [13].

On the basis of the experimental evidence collected so far, and reviewed in [16,17], the identification of these three resonances is a debated issue, and the experiments at BES III in Beijing, at the Jefferson Laboratory, the PANDA experiment at GSI, LHCb and COMPASS at CERN and the new Super-B factory at KeK will shed light on their actual existence and properties. Electroproduction studies can be found, for example, in [18]. If new hadronic states can be obtained explicitly considering the dynamics of gluonic excitations, hybrid configurations with non-exotic quantum numbers should also be present in the meson spectrum. However, their identification in this case is more difficult, due to the mixing with the ordinary $q\bar{q}$ configurations, and one has to mainly look for overpopulation of the levels with respect to, e.g., the quark model predictions. Candidates for hybrid non-exotic resonances are present in the charmonium system, namely $Y(4260)$ with $J^{PC} = 1^{--}$ [2].

[a] e-mail: floriana.giannuzzi@ba.infn.it

The properties of light and heavy hybrid mesons can be studied through different theoretical approaches. Focusing on the lightest 1^{-+} meson, using several phenomenological models some mass predictions have been obtained, which are around 1.5 GeV in the old bag model [19,20], in the range 1.7–1.9 GeV in the flux-tube model [21,22], within 1.8–2.2 GeV in a model with "constituent" gluon [23,24]. Using QCD sum rules, this mass is expected in the range 1.5–1.8 GeV [25–29], and the value $M = 1.73^{+0.10}_{-0.09}$ GeV is found in Ref. [30]. Lattice QCD analyses obtain $M(\pi_{1^{-+}}) = 1.74 \pm 0.25$ GeV [31] and $M \sim 2$ GeV [32]. Hence, the predictions of the mass of the lightest 1^{-+} meson drastically depend on the theoretical approach. With the exception of the bag model, a heavier mass with respect to the $\pi_1(1400)$ and $\pi_1(1600)$ hybrid candidates is generally predicted.

In the following, we study the light $J^{PC} = 1^{-+}$ hybrid states in a framework inspired by the gauge/string duality, using a holographic model of QCD able to describe several features of the low-energy strong interaction phenomenology [33]. We shall also analyse the differences with the outcome of another holographic QCD model, the so-called hard-wall model [34]. Moreover, we shall investigate the stability of the hybrid configurations against thermal effects in comparison with other hadrons with non-exotic quantum numbers.

2 Model

We adopt the so-called soft-wall model, introduced as a phenomenological approach to low-energy QCD inspired by the gauge/gravity correspondence [33]. The model aims at describing several nonperturbative features of QCD by a semiclassical theory living in a 5-dimensional anti-de Sitter space (AdS_5) assumed to be dual to QCD. The framework is inspired by the AdS/CFT correspondence, a conjecture relating type IIB string theory living in $AdS_5 \times S^5$ (S^5 is a 5-dimensional sphere) with $\mathcal{N} =$ Super-Yang Mills theory living in a 4-dimensional Minkowski space [35]. We use Poincaré coordinates with the line element of the AdS_5 space written as

$$ds^2 = \frac{R^2}{z^2}(dt^2 - d\bar{x}^2 - dz^2) \quad z > 0; \tag{1}$$

R is the radius of the AdS space, $(t, \mathbf{x})$ the ordinary 4-dimensional coordinates, and z the fifth holographic coordinate. Following the AdS/CFT correspondence dictionary [36,37], local gauge-invariant QCD operators with conformal dimension Δ can be described in the dual theory by proper fields, with mass of a p-form field fixed by the relation $m_5^2 R^2 = (\Delta - p)(\Delta + p - 4)$. The field dynamics and interactions are described by an action containing a background dilaton field introduced to break conformal invariance.

To describe hybrid 1^{-+} mesons, we use the QCD local operator $J^a_\mu = \bar{q} T^a G_{\mu\nu} \gamma^\nu q$, with $G_{\mu\nu}$ the gluon field strength and T^a flavour matrices normalised to $\mathrm{Tr}[T^a T^b] = \delta^{ab}/2$. This QCD operator has a dual field which is a 1-form, $H_\mu = H^a_\mu T^a$, with mass $m_5^2 R^2 = 8$. The dynamics of such a field is described by the Proca-like action (with AdS background):

$$S = \frac{1}{k} \int d^5x \sqrt{g} e^{-c^2 z^2} \times \mathrm{Tr}\left[-\frac{1}{4} F^{MN} F_{MN} + \frac{1}{2} m_5^2 H_M H^M \right], \tag{2}$$

with $F^{MN} = \partial_M H_N - \partial_N H_M$, and where M, N are 5-dimensional indices. g is the determinant of the metric (1) and k a parameter introduced to make the action dimensionless. The $e^{-c^2 z^2}$ factor introduces the mass parameter c breaking the conformal symmetry.

The Euler–Lagrange equations for the field $H^N(x, z)$, stemming from the action (2), are

$$\partial_M \left(\sqrt{g} e^{-c^2 z^2} F^{MN} \right) + \frac{8}{R^2} \sqrt{g} e^{-c^2 z^2} H^N = 0. \tag{3}$$

The H_μ field (Greek letters indicate 4-dimensional indices) can be decomposed in a longitudinal $H^\mu_\parallel$, and in a transverse $H^\mu_\perp$ component which satisfies the condition $\partial_\mu H^\mu_\perp = 0$ and can be used to describe the 1^{-+} mesons. From Eq. (3), the equation of motion for $H^\perp_\mu$ in the Fourier space is

$$\partial_z \left(\frac{e^{-c^2 z^2}}{z} \partial_z H^\perp_\mu \right) + q^2 \frac{e^{-c^2 z^2}}{z} H^\perp_\mu - 8 \frac{e^{-c^2 z^2}}{z^3} H^\perp_\mu = 0, \tag{4}$$

with mass spectrum and normalised eigenfunctions

$$q_n^2 = M_n^2 = 4c^2(n + 2), \tag{5}$$

$$H_n = \sqrt{\frac{2\,n!}{(n+3)!}} c^4 z^4 L_n^3(c^2 z^2), \tag{6}$$

(n integer and L_n^m the generalised Laguerre polynomial). This spectrum can be compared with the one of mesons with different quantum numbers and quark content, collected in Table 1. In all cases, linear Regge trajectories $M_n^2 \simeq n$ with the same slope are obtained, which was the main motivation for introducing the soft wall [33].

For the lightest hybrid state the result is $M_0^2 = 8c^2$ and setting c from the ρ meson mass and the relation in Table 1,

Table 1 Mass spectrum of $q\bar{q}$, glueballs and hybrids predicted in the soft-wall model

J^{PC}	1^{--} $(q\bar{q})$ [33]	0^{++} $(q\bar{q})$ [38]	0^{++} (glueball) [39]	1^{-+}
M_n^2	$c^2(4n+4)$	$c^2(4n+6)$	$c^2(4n+8)$	$c^2(4n+8)$

$c = M_\rho/2 = 388$ MeV, the value $M_0 \sim 1.1$ GeV is obtained. Other choices of c are possible. For example, one can fix c including the mass of the excited states of the 1^{--} spectrum, or the whole Regge trajectory, as done in [40]. In the latter case, we obtain $c \sim 474$ MeV and $M_0 \sim 1.34$ GeV. In any case, the value of the mass is always lower than the predictions obtained by other approaches, and favours $\pi_1(1400)$ rather than $\pi_1(1600)$ as the lightest 1^{-+} meson. A similar conclusion is drawn from the hard-wall model, in which the predicted mass of the lightest hybrid is $M_0 = 1476$ MeV [34]. The mass of the radial excitations can also be determined: the mass of the first radial excitation, in the soft-wall model, is given by $M_1/M_0 = \sqrt{3/2}$, while $M_1/M_0 = 2.61/1.476$ is found in the hard-wall model [34]. The difference between the two determinations of the mass of the first excited state underlines the main difference between the two models, the hard-wall model being characterised by the spectral condition $M_{n^2} \simeq n^2$.

Other properties can be extracted from the two-point correlation function

$$\Pi^{ab}_{\mu\nu} = i \int d^4x e^{iqx} \langle 0|T[J^a_\mu(x) J^b_\nu(0)]|0\rangle. \tag{7}$$

In the holographic approaches the computation of this quantity is based on the identification between the partition function of the conformal field theory and the one of the supergravity theory [36]. This allows one to get the two-point correlation function of an operator by functional derivation of the supergravity on-shell action with respect to the source of the operator. For the hybrid current operator, this relation can be written as

$$\Pi^{ab}_{\mu\nu}(q^2) = \left.\frac{\delta^2 S_{os}}{\delta H_0^{a\mu} \delta H_0^{b\nu}}\right|_{H_0=0}, \tag{8}$$

where $H^\mu_0(q^2)$ is the source in the Fourier space, related to the hybrid field $H^\mu(z,q) = H(z,q^2)H^\mu_0(q^2)$ by the bulk-to-boundary propagator $H(z,q^2)$. $\Pi^{ab}_{\mu\nu}(q^2)$ is the sum of a transverse and a longitudinal contribution:

$$\Pi^{ab}_{\mu\nu}(q^2) = -\left(\eta_{\mu\nu} - \frac{q_\mu q_\nu}{q^2}\right)\frac{\delta^{ab}}{2}\Pi^\perp(q^2) + \frac{q_\mu q_\nu}{q^2}\frac{\delta^{ab}}{2}\Pi^\parallel(q^2). \tag{9}$$

$H^\perp(z,q^2)$ is determined as the solution of Eq. (3) with boundary condition at small z: $H^\perp(z,q^2) = 1/z^2 + \mathcal{O}(z^0)$, and regular behaviour at $z \to \infty$:

$$H^\perp(z,q^2) = \frac{1}{2}\Gamma\left(2 - \frac{q^2}{4c^2}\right) z^{-2} \times U\left(-1 - \frac{q^2}{4c^2}, -2, c^2z^2\right), \tag{10}$$

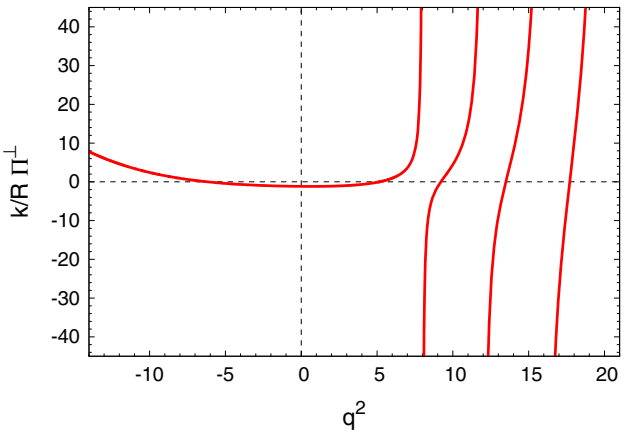

Fig. 1 $\Pi^\perp(q^2)$ in Eq. (11) (with $\epsilon = 1$)

in terms of the Tricomi confluent hypergeometric function $U(a,b,z)$. $\Pi^\perp(q^2)$ is given by $\Pi^\perp(q^2) = \frac{R}{k}\frac{e^{-c^2z^2}}{z} H^\perp(z,q^2)\partial_z H^\perp(z,q^2)\big|_{z=0}$, so that

$$\Pi^\perp(q^2) = \frac{R}{k}\left(-\frac{2}{\epsilon^6} + \frac{c^2 - q^2/4}{\epsilon^4} + \frac{c^2q^2}{4\epsilon^2} + \frac{1}{1152}\Big(- 192c^6 + 16c^4(-7 + 3\gamma_E)q^2 + 36c^2q^4 + (7 - 3\gamma_E)q^6 - 3q^2(-16c^4 + q^4) \times \left(HN\left(1 - \frac{q^2}{4c^2}\right) + 2\log(c\epsilon)\right)\Big)\right). \tag{11}$$

HN is the harmonic number function, and ϵ an inverse renormalisation scale. A plot of $\Pi^\perp(q^2)$ is shown in Fig. 1, setting $\epsilon = 1$.

The poles of $\Pi^\perp(q^2)$ reproduce the mass spectrum (5) with residues

$$F_n^2 = \frac{2Rc^8}{3k}(n+3)(n+2)(n+1). \tag{12}$$

The parameter k can be fixed by matching the leading-order perturbative QCD expression for $\Pi^\perp(Q^2)$ at $Q^2 = -q^2 \to \infty$ [25,26]

$$\Pi^\perp_{\rm QCD}(Q^2) = \frac{1}{960\pi^4}\log(Q^2)Q^6 \tag{13}$$

with the asymptotic $Q^2 \to \infty$ expansion of Eq. (11):

$$\Pi^\perp(Q^2) = \frac{R}{384k}\log(Q^2)Q^6, \tag{14}$$

obtaining $R/k = 2/(5\pi^4)$.

The results of this straightforward analysis are, therefore,

- the soft-wall model produces linear Regge trajectories also for the hybrid 1^{-+} states,
- a hierarchy with the vector and scalar glueball masses is found $M_\rho < M_G \simeq M_{1^{-+}}$,

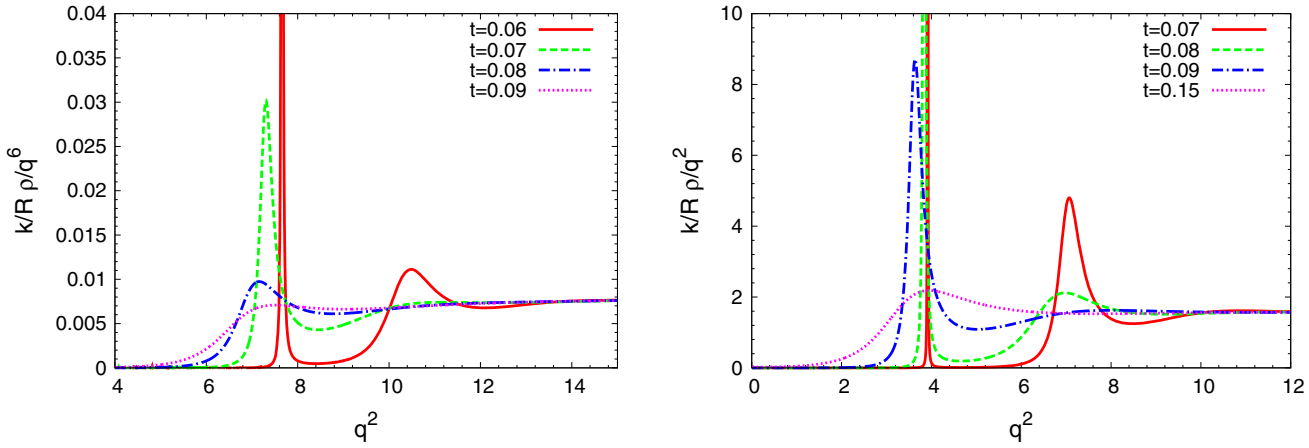

Fig. 2 *Left* (*right*) *panel*: spectral function of 1^{-+} (1^{--}) mesons at different values of temperature. The scale $c = 1$ has been set

- the expression for the residues is obtained,

which are interesting to compare with the outcome of different approaches.

3 Thermal effects on the hybrid meson spectrum

The soft-wall model allows a simple description of finite temperature effects on hadronic systems. An interesting quantity to study is the spectral function. For the hybrid states, at zero temperature the spectral function is represented by an infinite number of delta functions centred at the masses in (5). For vector mesons, scalar mesons and glueballs it has been found that on increasing the temperature these peaks broaden, and their positions move towards lower values[1] [41,42]. The analogous computation for hybrid mesons can be carried out.

Temperature can be incorporated in the holographic models introducing a black hole in the AdS space, with the position of its horizon z_h related to the (inverse) temperature, $z_h = 1/(\pi T)$. Now, the line element is

$$ds^2 = \frac{R^2}{z^2}\left(f(z)dt^2 - d\bar{x}^2 - \frac{dz^2}{f(z)}\right)$$
$$f(z) = 1 - z^4/z_h^4, \qquad 0 < z < z_h. \tag{15}$$

From the action (2), using the metric in (15), the equation of motion for a spatial component of the transverse field $H_i^{\perp}(z,q)$ can be obtained as in the $T = 0$ case:

$$\partial_z\left(\frac{e^{-c^2z^2}}{z}f(z)\partial_z H_i^{\perp}(z,q)\right) + \frac{e^{-c^2z^2}}{z}\left(\frac{q_0^2}{f(z)} - \bar{q}^2\right)$$
$$\times H_i^{\perp}(z,q) - 8\frac{e^{-c^2z^2}}{z^3}H_i^{\perp}(z,q) = 0; \tag{16}$$

[1] We are not considering in this discussion the possibility of a Hawking–Page transition [42].

we restrict ourselves to the meson rest-frame $\bar{q} = 0$. The bulk-to-boundary propagator is the solution of this equation with the same boundary condition at $z \to 0$ as in the $T = 0$ case ($H^{\perp}(z,q^2) = 1/z^2 + \mathcal{O}(z^0)$), while near the black-hole horizon an incoming-wave behaviour is required, $H^{\perp}(z,q^2) \sim (1 - z/z_h)^{-i\sqrt{q^2}z_h/4}(1 + \mathcal{O}(1 - z/z_h))$, to determine the retarded Green's function [43]:

$$\Pi_R(q^2) = \frac{R}{k}\frac{e^{-c^2z^2}f(z)}{z}H^{\perp}(z,q^2)\partial_z H^{\perp}(z,q^2)\Big|_{z\to 0}. \tag{17}$$

The resulting spectral function, the imaginary part of the retarded Green's function, is shown in Fig. 2 for a few values of temperature (in units of c: $t = T/c$). The broadening of the peaks and the shift of their position towards lower values when the temperature is increased, are clearly visible. The temperature dependence of the mass and width of the lowest lying state, determined fitting the spectral function by a Breit–Wigner formula,

$$\rho(\omega^2) = \frac{a\, m\, \Gamma\, \omega^b}{(\omega^2 - m^2)^2 + m^2\Gamma^2} \tag{18}$$

with parameters a and b, is depicted in Fig. 3. We determine the melting temperature $t \sim 0.10$ for the hybrid meson looking at the value of t where the peak in the spectral function is reduced by a factor $\simeq$ 15–20 with respect to the point where the width starts to broaden ($t \simeq 0.065$), a criterium already adopted in [42].

In Fig. 2 we also plot, for comparison, the spectral function of vector mesons ($J^{PC} = 1^{--}$). This shows that, although the general behaviour of the spectral function with temperature is similar, hybrid states are more unstable than 1^{--} states and melt at lower temperatures.

Vector mesons melt at $t \sim 0.23$ [44,45], while scalar glueballs melt at $t \sim 0.12$ [42], as specified in Table 2. The dif-

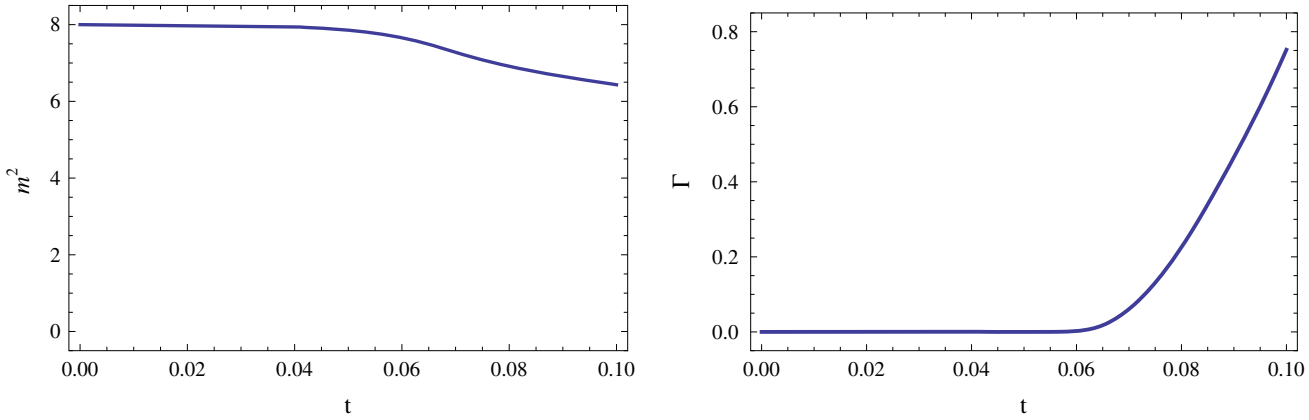

Fig. 3 Squared mass (*left*) and width (*right*) of the lightest 1^{-+} meson at increasing temperature (with $c = 1$)

Table 2 Melting temperature of $q\bar{q}$, glueball and hybrid states predicted in the soft-wall model

J^{PC}	1^{--} $(q\bar{q})$ [44,45]	$0^{++}(q\bar{q})$ [42]	0^{++} (glueball) [42]	1^{-+}
$t = T/c$	0.23	0.18	0.12	0.10

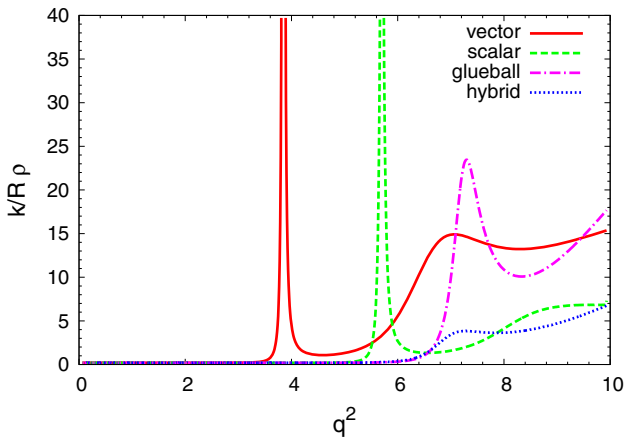

Fig. 4 Spectral functions of vector mesons, scalar mesons, scalar glueballs and 1^{-+} hybrid mesons at $t = 0.08$, setting the scale $c = 1$

ferent response to temperature of the various hadronic states can be appreciated considering Fig. 4, in which the spectral functions of states with different quantum numbers are computed at the same temperature $t = 0.08$.

The dissociation temperature of the hybrid mesons can also be determined computing the potential in the Schrödinger-like equation to which Eq. (16) can be transformed. The tortoise coordinate r can be defined, such that $\partial_r = -f(z)\partial_z$:

$$r = \frac{z_h}{2}\left(-\arctan\left(\frac{z}{z_h}\right) + \frac{1}{2}\ln\left(\frac{z_h - z}{z_h + z}\right)\right). \tag{19}$$

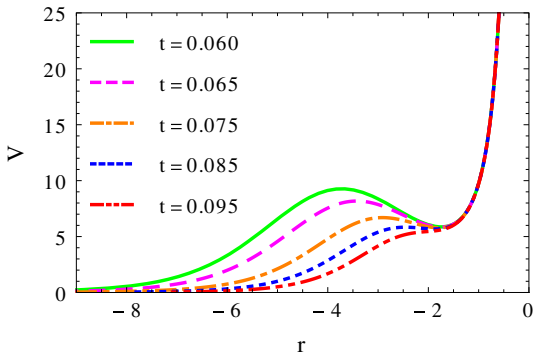

Fig. 5 Potential V vs. the tortoise coordinate r for several values of the temperature ($c = 1$)

After a redefinition of the field $H^{\perp} = \sqrt{z}e^{c^2z^2/2}\psi$, Eq. (16), with $\bar{q} = 0$, can be written as

$$-\psi''(r, q_0^2) + V(z(r))\psi(r, q_0^2) = q_0^2\psi(r, q_0^2), \tag{20}$$

with the potential

$$V(z) = \frac{f(z)}{z^2}\left(c^4z^4f(z) + \frac{4c^2z^6}{z_h^4} + \frac{35}{4} + \frac{5}{4}\frac{z^4}{z_h^4}\right) \tag{21}$$

in which the dependence on the temperature (through the horizon position) is explicit. The variation of the potential with temperature is shown in Fig. 5. At a critical temperature the r dependence of the potential becomes monotonous, so that no bound states can be formed. Such a temperature coincides with the one inferred from the spectral function.

4 Conclusions

We have computed the spectrum and the decay constants of 1^{-+} hybrid mesons in the soft-wall holographic model of QCD. For the lowest-lying state we have found $M \sim 1.1-1.3$

GeV, depending on the mass scale c. This value is close to the mass of $\pi_1(1400)$, the lightest one of the hybrid candidates. The behaviour of 1^{-+} hybrid mesons at finite temperature has been studied, showing that dissociation occurs at a much lower temperature than for 1^{--} mesons, and also at a lower temperature than in the case of other kind of hadrons. This result can be interpreted as an indication that hybrid quark-gluon configurations, although present in the meson spectrum, suffer from larger instabilities with respect to the conventional configurations, and this could explain the difficulty in their detection in actual conditions, i.e. both in the finite number of colour condition ($N_c = 3$), which is different from the holographic one holding in the large N_c limit, and in the experimental environment.

Acknowledgments We thank M. Battaglieri, F. De Fazio and S. Nicotri for fruitful discussions.

References

1. For a review see C. Amsler, N.A. Tornqvist, Phys. Rept. 389, 61 (2004)
2. E.S. Swanson, Phys. Rept. **429**, 243 (2006)
3. D.R. Thompson et al., E852 Collaboration. Phys. Rev. Lett. **79**, 1630 (1997)
4. S.U. Chung et al., E852 Collaboration. Phys. Rev. D **60**, 092001 (1999)
5. A. Abele et al., Crystal Barrel Collaboration. Phys. Lett. B **423**, 175 (1998)
6. A. Abele et al., Crystal Barrel Collaboration. Phys. Lett. B **446**, 349 (1999)
7. P. Salvini et al., OBELIX Collaboration. Eur. Phys. J. C **35**, 21 (2004)
8. G.S. Adams et al., E862 Collaboration. Phys. Lett. B **657**, 27 (2007)
9. J. Beringer et al., Particle Data Group Collaboration. Phys. Rev. D **86**, 010001 (2012)
10. G.S. Adams et al., E852 Collaboration. Phys. Rev. Lett. **81**, 5760 (1998)
11. E.I. Ivanov et al., E852 Collaboration. Phys. Rev. Lett. **86**, 3977 (2001)
12. J. Kuhn et al., E852 Collaboration. Phys. Lett. B **595**, 109 (2004)
13. M. Lu et al., E852 Collaboration. Phys. Rev. Lett. **94**, 032002 (2005)
14. M. Alekseev et al., COMPASS Collaboration. Phys. Rev. Lett. **104**, 241803 (2010)
15. B.A. Mecking et al., CLAS Collaboration. Nucl. Instrum. Meth. A **503**, 513 (2003)
16. B. Ketzer, PoS QNP **2012**, 025 (2012)
17. D. Bettoni, PoS BORMIO **2012**, 004 (2012)
18. I.V. Anikin, B. Pire, L. Szymanowski, O.V. Teryaev, S. Wallon, Phys. Rev. D **70**, 011501 (2004)
19. M.S. Chanowitz, S.R. Sharpe, Nucl. Phys. B 222, 211 (1983). [Erratum-ibid.B 228, 588 (1983)]
20. T. Barnes, F.E. Close, F. de Viron, J. Weyers, Nucl. Phys. B **224**, 241 (1983)
21. N. Isgur, J.E. Paton, Phys. Rev. D **31**, 2910 (1985)
22. T. Barnes, F.E. Close, E.S. Swanson, Phys. Rev. D **52**, 5242 (1995)
23. S. Ishida, H. Sawazaki, M. Oda, K. Yamada, Phys. Rev. D **47**, 179 (1993)
24. I.J. General, S.R. Cotanch, F.J. Llanes-Estrada, Eur. Phys. J. C **51**, 347 (2007)
25. I.I. Balitsky, D. Diakonov, A.V. Yung, Z. Phys, C **33**, 265 (1986)
26. I.I. Balitsky, D. Diakonov, A.V. Yung, Phys. Lett. B **112**, 71 (1982)
27. J.I. Latorre, P. Pascual, S. Narison, Z. Phys, C **34**, 347 (1987)
28. K.G. Chetyrkin, S. Narison, Phys. Lett. B **485**, 145 (2000)
29. S. Narison, Phys. Lett. B **675**, 319 (2009)
30. Z.-F. Zhang, H.-Y. Jin, T.G. Steele. arXiv:1312.5432 [hep-ph]
31. J.N. Hedditch, W. Kamleh, B.G. Lasscock, D.B. Leinweber, A.G. Williams, J.M. Zanotti, Phys. Rev. D **72**, 114507 (2005)
32. J.J. Dudek, Phys. Rev. D **84**, 074023 (2011)
33. A. Karch, E. Katz, D.T. Son, M.A. Stephanov, Phys. Rev. D **74**, 015005 (2006)
34. H.-C. Kim, Y. Kim, JHEP **0901**, 034 (2009)
35. J.M. Maldacena, Adv. Theor. Math. Phys. **2**, 231 (1998)
36. E. Witten, Adv. Theor. Math. Phys. **2**, 253 (1998)
37. S.S. Gubser, I.R. Klebanov, A.M. Polyakov, Phys. Lett. B **428**, 105 (1998)
38. P. Colangelo, F. De Fazio, F. Giannuzzi, F. Jugeau, S. Nicotri, Phys. Rev. D **78**, 055009 (2008)
39. P. Colangelo, F. De Fazio, F. Jugeau, S. Nicotri, Phys. Lett. B **652**, 73 (2007)
40. O. Andreev, V.I. Zakharov, Phys. Rev. D **74**, 025023 (2006)
41. M. Fujita, K. Fukushima, T. Misumi, M. Murata, Phys. Rev. D **80**, 035001 (2009)
42. P. Colangelo, F. Giannuzzi, S. Nicotri, Phys. Rev. D **80**, 094019 (2009)
43. D.T. Son, A.O. Starinets, JHEP **0209**, 042 (2002)
44. L.A.H. Mamani, A.S. Miranda, H. Boschi-Filho, N.R.F. Braga. arXiv:1312.3815 [hep-th]
45. A.S. Miranda, C.A. Ballon Bayona, H. Boschi-Filho, N.R.F. Braga, JHEP **0911**, 119 (2009)